

NO-A103 694

RELATIONSHIP OF SURFACE ACOUSTIC WAVE VAPOR SENSOR
RESPONSES TO THERMODYN. (U) NAVAL RESEARCH LAB
WASHINGTON DC J W GRATE ET AL. 29 JUL 87 NRL-MR-6024

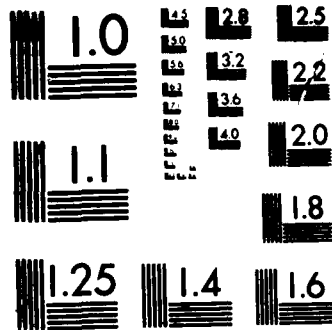
1/1

UNCLASSIFIED

F/G 7/6

NL

									END			
									9-87			
									DTIC			



MICROCOPY RESOLUTION TEST CHART
NATIONAL BUREAU OF STANDARDS-1963-A

AD-A183 694

**Relationship of Surface Acoustic Wave Vapor
Sensor Responses to Thermodynamic Parameters for
Gas Solubility: Polymer/Gas Partition Coefficients
for Fluoropolyol**

J. W. GRATE AND A. SNOW

*Surface Chemistry Branch
Chemistry Division*

D. S. BALLANTINE

*GEO Centers, Inc.
Fort Washington, MD 20744*

H. WOHLTJEN

*Microsensors Systems Inc.
Fairfax, VA 22030*

M. H. ABRAHAM, A. R. MCGILL AND P. SASSON

*University of Surrey
Guildford Surrey GU2 5XH
United Kingdom*

July 29, 1987

Approved for public release; distribution unlimited.

SDTIC
ELECTE
AUG 2 1 1987
S D
Cly D.

REPORT DOCUMENTATION PAGE

1a. REPORT SECURITY CLASSIFICATION UNCLASSIFIED		1b. RESTRICTIVE MARKINGS	
2a. SECURITY CLASSIFICATION AUTHORITY		3. DISTRIBUTION/AVAILABILITY OF REPORT Approved for public release; distribution unlimited.	
2b. DECLASSIFICATION/DOWNGRADING SCHEDULE		5. MONITORING ORGANIZATION REPORT NUMBER(S)	
4. PERFORMING ORGANIZATION REPORT NUMBER(S) NRL Memorandum Report 6024		7a. NAME OF MONITORING ORGANIZATION	
6a. NAME OF PERFORMING ORGANIZATION Naval Research Laboratory	6b. OFFICE SYMBOL (if applicable) Code 6170	7b. ADDRESS (City, State, and ZIP Code)	
6c. ADDRESS (City, State, and ZIP Code) Washington, DC 20375-5000		9. PROCUREMENT INSTRUMENT IDENTIFICATION NUMBER	
8a. NAME OF FUNDING/SPONSORING ORGANIZATION Chemical Research Development & Engineering Ctr.	8b. OFFICE SYMBOL (if applicable) CRDEC	10. SOURCE OF FUNDING NUMBERS	
8c. ADDRESS (City, State, and ZIP Code) Aberdeen Proving Ground Aberdeen, MD 21010-5423		PROGRAM ELEMENT NO.	PROJECT NO.
		TASK NO.	WORK UNIT ACCESSION NO. DN180-445
11. TITLE (Include Security Classification) Relationship of Surface Acoustic Wave Vapor Sensor Responses to Thermodynamic Parameters for Gas Solubility: Polymer/Gas Partition Coefficients for Fluoropolyol			
12. PERSONAL AUTHOR(S) (See page ii)			
13a. TYPE OF REPORT Memorandum	13b. TIME COVERED FROM TO	14. DATE OF REPORT (Year, Month, Day) 1987 July 29	15. PAGE COUNT 50
16. SUPPLEMENTARY NOTATION *GEO Center, Inc., Ft. Washington, MD 20744, **Microsensors Systems, Inc., Fairfax, VA 22030 ***University of Surrey, Guildford, Surrey GU2 5XH, United Kingdom			
17. COSATI CODES		18. SUBJECT TERMS (Continue on reverse if necessary and identify by block number)	
FIELD	GROUP	Surface acoustic wave, Vapor sensor, Fluoropolyol, Partition coefficient, Microsensor, Gas liquid chromatography	
19. ABSTRACT (Continue on reverse if necessary and identify by block number) Surface acoustic wave (SAW) devices coated with a thin film of a stationary phase sense chemical vapors in the gas phase by detecting the mass of the vapor which distributes into the stationary phase. This distribution can be described by the partition coefficient, which gives the ratio of the concentration of the vapor in the stationary phase to the concentration of the vapor in the gas phase. An equation is presented which allows partition coefficients to be calculated from SAW vapor sensor frequency shifts. Partition coefficients for nine vapors into SAW coating "fluoropolyol" have been determined by this method, using both 112 MHz and 158 MHz SAW devices. Partition coefficients have also been determined independently by GLC and the results are in good agreement. The relationship between SAW frequency shifts and partition coefficients allows SAW sensor responses to be predicted if the partition coefficient has been measured by GLC, or if the partition coefficient can be estimated by various correlation methods being developed.			
20. DISTRIBUTION/AVAILABILITY OF ABSTRACT <input checked="" type="checkbox"/> UNCLASSIFIED/UNLIMITED <input type="checkbox"/> SAME AS RPT. <input type="checkbox"/> DTIC USERS		21. ABSTRACT SECURITY CLASSIFICATION UNCLASSIFIED	
22a. NAME OF RESPONSIBLE INDIVIDUAL Jay W. Grate		22b. TELEPHONE (Include Area Code) (202) 767-2536	22c. OFFICE SYMBOL Code 6170

12. PERSONAL AUTHOR(S)

Grate, Jay W., Snow, Arthur, Ballantine, David S.,* Wohltjen, Hank,** Abraham,***
Michael H., McGill,*** Andrew R., Sasson,*** Pnina

CONTENTS

INTRODUCTION	1
EXPERIMENTAL	5
Materials	5
112 MHz SAW Device	5
158 MHz SAW Device	6
Vapor Sensor Coating	7
Vapor Stream Generation	8
Sensor Response Data Collection	8
Gas Liquid Chromatography (GLC)	10
RESULTS	11
Equation Relation SAW Frequency Shift to Partition Coefficient	11
Relationship to Thermodynamic Parameters for Gas Solubility	14
K Values Determined from SAW Vapor Sensor Frequency Shifts	15
K Values Determined by GLC Measurements	28
DISCUSSION	30
CONCLUSIONS	38
ACKNOWLEDGMENTS	39
REFERENCES	40
APPENDIX	42

Accession For	
NTIS CRA&I	<input checked="" type="checkbox"/>
DTIC TAB	<input type="checkbox"/>
Unannounced	<input type="checkbox"/>
Justification	
By	
Distribution /	
Availability Codes	
Dist	Avail. and/or Special
A-1	



RELATIONSHIP OF SURFACE ACOUSTIC WAVE VAPOR SENSOR RESPONSES
TO THERMODYNAMIC PARAMETERS FOR GAS SOLUBILITY:
POLYMER/GAS PARTITION COEFFICIENTS FOR FLUOROPOLYOL

INTRODUCTION

The use of surface acoustic wave (SAW) devices for sensing chemical vapors in the gas phase was first reported in 1979,¹ and has since been investigated by several groups.²⁻¹⁰ SAW devices function by generating mechanical Rayleigh surface waves on a thin slab of a piezoelectric material (such as quartz) and oscillate at a characteristic resonant frequency when placed in an oscillator circuit with an rf amplifier.⁶ The oscillator frequency is measurably altered by small changes in mass or elastic modulus at the surface of the SAW device. Vapor sensitivity is typically achieved by coating the device surface with a thin film of a stationary phase which will selectively absorb and concentrate the target vapor. Vapor sorption increases the mass of the surface film and a shift in the oscillator frequency is observed. SAW devices offer many advantages as chemical sensors including small size, low cost, ruggedness, and high sensitivity. A further advantage is the potential for these devices to be adapted to a variety of gas phase analytical problems by strategic design or selection of coating material. Full realization of this potential will require methods to quantify, understand, and finally to predict the vapor/coating interactions responsible for vapor sorption.

The change in oscillator frequency, Δf_s , observed when a bare SAW device is coated with an isotropic, non piezoelectric, thin film has been described by equation (1).⁶

$$\Delta f_s = (k_1 + k_2) F^2 h \rho - k_2 F^2 h \left(\frac{4\mu}{V_r^2} \left(\frac{\lambda + \mu}{\lambda + 2\mu} \right) \right) \quad (1)$$

k_1 and k_2 are material constants for the piezoelectric substrate; F is unperturbed resonant frequency of the SAW oscillator, which is determined by the geometry of the interdigital transducers fabricated onto the surface; h is the coating thickness; ρ is the coating density; μ and λ are the shear modulus and Lamé constants of the coating; and V_r is the Rayleigh wave velocity in the piezoelectric substrate. The second term in this equation depends on the mechanical properties of the film, and is often negligible for soft organic materials. If the mechanical properties are negligible, then equation (1) reduces to equation (2), which describes the perturbation in frequency caused by the mass of the applied film⁶ ($h\rho$ is simply the mass per unit area of the film). This treatment assumes 100% coverage of the device active area.

$$\Delta f_s = (k_1 + k_2) F^2 h \rho \quad (2)$$

Similarly, the frequency shift observed when the coated SAW device is exposed to a vapor provides a measure of the mass of the vapor absorbed.

Sorption of ambient vapor into the SAW device coating until equilibrium is reached represents a partitioning of the solute vapor between the gas phase and the stationary phase. This process is illustrated in Figure 1. The distribution can be quantified by a partition coefficient, K , which gives the ratio of the concentration of the vapor in the stationary phase, C_s , to the concentration of the vapor in the vapor phase, C_v (equation 3).

$$K = \frac{C_s}{C_v} \quad (3)$$

An equation is derived herein which allows K to be calculated directly from observed SAW vapor sensor frequency shifts. This conversion provides a standardized method of normalizing empirical SAW data, and does so in a way that provides information about the vapor/coating equilibrium.

In this study we examine in detail the absorption of vapors into a soft polymeric material referred to as "fluoropolyol". This material was chosen on the basis of a prior study where several diverse stationary phases were applied to SAW devices and exposed to a range of chemical vapors.³ The fluoropolyol-coated sensor gave some of the highest responses observed. We now present vapor response data for fluoropolyol coated onto both 112 and 158 MHz SAW devices. These data have been used to calculate partition coefficients for each vapor into fluoropolyol. Partition coefficients for the same vapors into fluoropolyol were

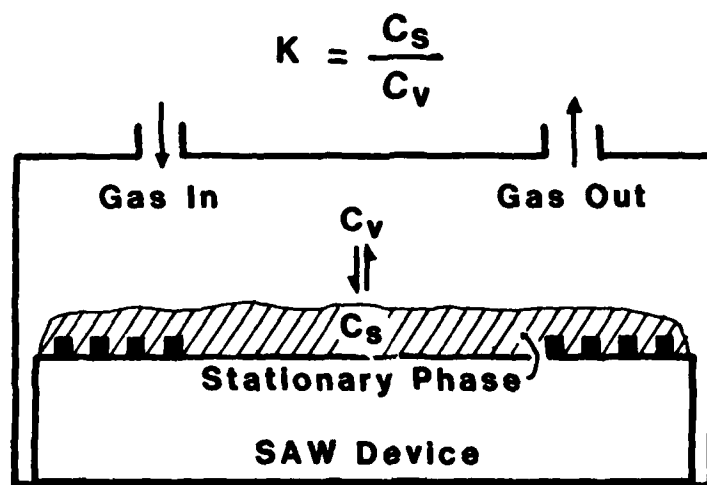


Figure 1. The distribution of vapor between the gas phase and the stationary phase which is quantified by the partition coefficient, K .

also determined independently by gas-liquid chromatographic (GLC) measurements. The values resulting from these two different techniques are in good agreement.

These results demonstrate that the mechanism of action of a coated SAW device is the same as that of GLC, i.e., reversible absorption of the vapor in the gas phase into the stationary phase. This confirms the solubility model for the interaction of vapors with the SAW coating; i.e. the solute vapor dissolves and distributes into the solvent stationary phase. Finally, the correlation between SAW vapor sensor responses and GLC partition coefficients creates a means for predicting SAW sensor behavior. Thus, if GLC partition coefficients are available from experimental measurement, or can be reliably predicted, then SAW vapor sensor responses can also be predicted.

EXPERIMENTAL

Materials. The fluoropolyol used in these studies was synthesized and provided by Dr. Jim Griffith of the Naval Research Laboratory Polymeric Materials Branch. These types of materials are prepared by methods described by O'Rear et. al.¹¹ The density of the fluoropolyol could not be determined using a density bottle or a pycnometer because of its high viscosity. Instead, a bulb with a vertical calibrated stem was weighed before and after being filled with fluoropolyol. On leaving the device in a thermostat, the polymer gradually settled and the volume reading was then taken. The results at various

temperatures are as follows: $T(^{\circ}\text{C}), \rho(\text{g ml}^{-1})$; 25, 1.6530; 40, 1.6322; 60, 1.6044; 90, 1.5629. The glass transition temperature of fluoropolyol is 10°C .

The liquid solvents used to generate vapor streams were commercial materials of greater than 99% purity, except diethyl sulfide (98%, Aldrich) and dimethyl methylphosphonate (DMMP) (97%, Aldrich). The solutes used in the GLC measurements were also commercial materials used as received; the GLC method does not require highly purified compounds.

112 MHz SAW Device. The 112 MHz dual SAW delay line sensors (Microsensor Systems, Inc. part number SD-112-B) were fabricated photolithographically using gold electrode metallization onto polished ST cut quartz substrates (1 cm x 1 cm x 0.08 cm thick). Each interdigital transducer (IDT) consisted of 50 finger pairs having one quarter wavelength finger widths and spacings (7 microns) and an 80 wavelength (.2240 cm) acoustic aperture. The IDT's were separated by 264 wavelengths (0.7392 cm). These 112 MHz SAW devices differ from those described previously³ in having a separate ground contact for each IDT. Electrical contacts from the RF electronics to the IDT contact pads were made by mounting the device in a plastic box with small gold-plated clips and screws. The lid to the box was equipped with two stainless steel tubes for the vapor stream inlet and outlet.

Each delay line was connected to a TRW model CA2820 wideband RF amplifier to provide the amplification necessary for oscillation to occur. The frequencies obtained from each

oscillator were mixed in a double balanced mixer (Mini Circuits Labs SRA-1) to provide a low frequency difference signal between the two delay lines on the device.

150 MHz SAW Device

The 150 MHz dual SAW devices used in this study (Microsensor Systems, Inc. part number SD-150-A) were also fabricated on ST cut quartz substrates. The two delay lines were lithographically patterned onto a chip that was approximately 0.5 cm square. This chip was epoxied onto a conventional gold plated, 12 pin, TO-8 style integrated circuit package and electrical connections were made from the SAW interdigital electrodes by means of ultrasonically welded 1 mil gold wires. After coating the device, the device was covered and sealed by a nickel plated lid with two 1/16 inch stainless steel tubes for vapor flow. The input interdigital transducer for each SAW device consisted of 75 pairs of electrodes with each pair repeated at 20 micron intervals (i.e. an acoustic wavelength of 20 microns). The acoustic aperture was 70 wavelengths (i.e. 0.1400 cm). The output interdigital transducer was spaced 10 wavelengths (i.e. 0.0200 cm) from the input transducer and consisted of 100 pairs of electrodes also having each pair repeated at 20 micron intervals. The edges of the quartz substrate beyond the ends of the delay lines were cut 5° out of parallel with the IDT fingers to eliminate triple transit echos. Coatings applied to the device covered the entire surface of the electrodes as well as the space in between electrodes.

Vapor Sensor Coating. Vapor sensors were prepared by coating one delay line with a thin film of fluoropolyol. The uncoated delay line served as a reference oscillator to provide temperature and pressure compensation. The coating was applied by spraying a dilute solution of fluoropolyol in chloroform through a small mask positioned to shield the reference delay line. The spray was generated with an airbrush using compressed air as the propellant. The difference frequency of the device was monitored until the desired amount of coating had been applied.

The two 112 MHz sensors reported herein were coated with 106 and 104 KHz of film respectively. The first was coated and stored overnight in ambient air prior to vapor testing. The second was annealed for one hour at 110°C and stored overnight in ambient air prior to vapor testing. After the first round of vapor testing, these devices were stored for two months in ambient air and then tested again.

The 158 MHz SAW device was coated with 207 KHz of film and stored for one week at room temperature prior to vapor testing.

Vapor stream generation. Vapor streams were generated from gravimetrically calibrated permeation tubes or gravimetrically calibrated bubblers using an automated vapor-generation instrument described in reference 12. This instrument generates selected vapor streams, dilutes them, and delivers a programmable flow rate of either clean carrier gas or the diluted vapor stream to the sensor. The instrument is controlled with an Apple IIe computer.

For these studies the carrier gas was dry air delivered to the sensor at ambient pressure. Dimethyl methylphosphonate and N,N-dimethylacetamide vapor streams were generated using permeation tubes and the remaining vapor streams were generated from bubblers. The flow rate of vapor stream to the sensor was 100mL/min.

In between collecting the first data sets on the 112 MHz devices and collecting the aged data set on the 112 MHz devices, the handling of permeation tubes was changed in a manner which appears to affect the concentrations generated. The 158 MHz data were also collected after this change. In the first data set permeation tube chambers were flushed for one hour prior to vapor testing to remove accumulated vapor. Normally the chambers were closed. This procedure was changed so that the chambers are continually flushed, 24 hours a day, assuring equilibrium conditions in each chamber at all times.

Vapor concentrations are calculated from the mass flow of the permeation tube as measured under equilibrium conditions. If one hour of flushing did not assure equilibrium conditions and remove buildup of vapor in the chamber or on the chamber walls, then the delivered concentrations may have been higher than the concentrations assigned based on the mass flow rates determined from the weight loss of the permeation tube. This would result in higher apparent frequency shifts and K_{saw} values. The log K values reported for DMMP and DMAC prior to continual permeation tube flushing are in parentheses in the tables.

Sensor response data collection. The difference frequency from the SAW sensor was monitored using a Systron-Donner model 6042A frequency counter or with a Phillips PM6674 frequency counter. The data were transferred over an IEEE-488 bus to an Apple IIe computer. This computer was in communication with the computer controlling vapor stream flows so that data collection and vapor stream operations were synchronized. The frequency data were collected at 1 Hz resolution. The difference in the frequency before the sensor was exposed to the vapor stream (i.e. the sensor is under clean dry air) and after the sensor has reached a stable equilibrium response to the vapor stream gives the frequency shift caused by the vapor.

The observed frequency shifts were used to calculate a partition coefficient for each vapor exposure. However, frequency shifts of less than 100-200 Hz were generally omitted from subsequent calculations so that K values were determined only from sensor responses with high signal to noise ratios.

Gas liquid chromatography (GLC). Fluoropolyol-gas partition coefficients, defined by equation 3, were obtained by GLC using fluoropolyol as the stationary phase. Absolute values of K (denoted by us previously as L)¹³ were obtained essentially as described before,¹³ using glass columns 1.5 m long containing a 4% loading of fluoropolyol on chromosorb GAW, with helium as the carrier gas and a thermal conductivity detector. Corrections for the pressure drop across the column were made as described (see equations 4-6 in ref. 13), and corrections for gas imperfections (equation 7 in ref. 13) were

also carried out. However, the latter were trivial. Two series of measurements, at 298°K and at 333°K, with alcohols as the standard solutes were carried out: results are in Table VI. Values of K for water were also obtained. A variety of solutes were then examined at both 298°K and 333°K, using a flame ionization detector, and relative values of K were converted to absolute values, using the known absolute values of the standard compounds, exactly as described before.¹³

RESULTS

Equation Relating SAW Frequency Shift to Partition Coefficient

The derivation of an equation relating SAW frequency shifts directly to partition coefficients begins with equation (2), which gives the frequency shift caused by a thin film on the SAW surface. The product of the factors h (film thickness in m) and ρ (film density in kg m^{-3}) in this equation is simply the mass per unit area.⁶ Therefore the frequency shift in Hz, Δf_s caused by application of the thin film coating onto the bare SAW device can be expressed as in equation (4).

$$\Delta f_s = \frac{(k_1 + k_2) F^2 m_s}{A} \quad (4)$$

The variable m_s is the mass of the coating in kg and A is the coated area in m^2 . The frequency shift in Hz, Δf_v , caused by absorption of the vapor into the coating can be expressed similarly as in equation (5).

$$\Delta f_v = \frac{(k_1+k_2)F^2m_v}{A} \quad (5)$$

The variable m_v is the mass of the vapor in the stationary phase coating. Division of equation (5) by equation (4) and rearranging gives equation (6).

$$\Delta f_v = \Delta f_s \frac{m_v}{m_s} \quad (6)$$

The mass of the vapor in the stationary phase coating is the factor of greatest interest. It can be related to the concentration of the vapor in the stationary phase C_s , in grams per liter, by equation (7).

$$C_s = \frac{m_v}{V_s (.001 \text{ kg g}^{-1})} \quad (7)$$

V_s is the volume of the stationary phase in liters. Now, substitution of (7) into (3) and rearranging gives (8).

$$m_v = K C_v V_s (.001 \text{ kg g}^{-1}) \quad (8)$$

C_v is the concentration of the vapor in the gas phase in grams per liter. Finally, substitution of (8) into (6) relates Δf_v to K as shown in equation (9).

$$\Delta f_v = \frac{\Delta f_s K C_v V_s (.001 \text{ kg g}^{-1})}{m_s} \quad (9)$$

This result can be further simplified by noting that V_s/m_s is the reciprocal of the density, ρ , of the stationary phase. If Δf_s is converted from Hz to KHz, the .001 conversion factor cancels out. The final result is equation (10):

$$\Delta f_v = \frac{\Delta f_s C_v K}{\rho} \quad (10)$$

Δf_v = vapor frequency shift ;in Hz

Δf_s = coating frequency shift in KHz

ρ = coating density in kg L^{-1} (= g mL^{-1})

C_v = vapor concentration in the gas phase in g L^{-1}

K = partition coefficient

The assumptions inherent in equation (10) are that the SAW device functions as a mass sensor (mechanical effects are negligible) and that the observed mass change is due to partitioning of the vapor between the gas phase and the stationary phase coating. In this regard, the equation represents a solubility model, i.e. dissolution of the solute vapor into the solvent stationary phase. The partition coefficient, K , can be readily calculated since all the remaining

terms are known. Δf_s is determined when the vapor sensitive coating of density ρ is applied to the bare SAW device. Δf_v is measured when the sensor is exposed to a calibrated vapor stream of concentration C_v . The units of C_v , $g L^{-1}$, are appropriate since dynamic vapor streams are typically prepared by diluting a measured mass flow ($g \text{ min}^{-1}$) into a known volumetric flow ($L \text{ min}^{-1}$) of carrier gas.¹²

One additional assumption is made in the substitution of the reciprocal of the stationary phase density, ρ , for V_s/m_s in equation (9). Following the derivation closely it is seen that m_s is the mass of the stationary phase, whereas V_s is the volume of the stationary phase when an equilibrium quantity of vapor has been absorbed. This volume is therefore assumed to be equal to the volume of the stationary phase itself. So long as the mass loading of the stationary phase by vapor is low, as it will be for low vapor concentrations or weakly sorbed vapors, this assumption is reasonable. In addition, the density of the material applied as a thin film is taken to be the same as the density of the bulk material.

Relationship to Thermodynamic Parameters for Gas Solubility

Equation (3) is a standard equation for the expression of gas solubility in a liquid at a constant temperature. The limiting value of the partition coefficient at low concentration may be defined as

$$K^\circ = \left(\frac{C_s}{C_v} \right)_{C \rightarrow 0} \quad (11)$$

and under normal gas chromatographic conditions, derived values of the gas-liquid partition coefficient may be taken as identical to K° . It should be pointed out that K° is the same as the Ostwald solubility coefficient, L° , defined exactly as in equation (11). Hence if equation (10) is applied to the detection of gases or vapors at low partial pressures, the constant K should represent K° (or L°).

The Henry's constant for absorption of a gas in a liquid at again limiting concentration or partial pressure, is defined as

$$K^H = \left(\frac{P_V}{X_S} \right)_{P_V \rightarrow 0} \quad (12)$$

where P_V is the solute partial pressure and X_S the solute mole fraction in the liquid phase. Since K^H and K° are related through equation (13), it is easy to derive an equation that connects Δf_V and K^H .

$$K^H = RT_\rho / M_S K^\circ \quad (13)$$

However, such an equation will be rigorously true only for liquid stationary phases whose molecular weight, M_S , is known. In the present context, using polymeric stationary phases, the relationship is of little value.

K values Determined from SAW Vapor Sensor Frequency Shifts.

Vapor response data were collected using 112 or 158 MHz SAW dual delay line sensors with one delay line coated with a thin film of

fluoropolyol. These devices are shown schematically in Figures 2 and 3. The chemical structure of fluoropolyol is shown in Figure 4. Coating a delay line with a thin film causes its frequency of oscillation to decrease in accordance with equation (2). The magnitude of this decrease provides a measure of the amount of coating applied.⁶ For example, 112 MHz SAW devices are typically coated with sufficient material to produce a 100 KHz frequency decrease in the coated delay line. Using equation (2), the 1.653 g mL⁻¹ density of fluoropolyol, and values of -9.33×10^{-8} and -4.16×10^8 m² sec kg¹ for k_1 and k_2 ,⁶ the estimated average thickness of a 100 KHz film of fluoropolyol on a 112 MHz SAW device is 36 nm. Given that the active area of the device is 0.17 cm², this corresponds to about 1 μg of material on the active surface. Similarly, a 158 MHz device with 200 KHz of fluoropolyol has an average coating thickness of 36 nm.

When a SAW vapor sensor under clean air is exposed to air containing a vapor to which it is sensitive, the frequency of the coated delay line shifts from its baseline value to a still lower frequency. This causes the measured difference frequency between the coated and uncoated delay lines to increase. A typical response curve for two successive vapor exposures is shown in Figure 5.

For most of the vapors at the concentrations employed in these studies, the frequency shifts were less than a few thousand Hz on the 112 MHz sensors. For water and isooctane, the highest shifts were less than one thousand Hz. For strongly sorbed

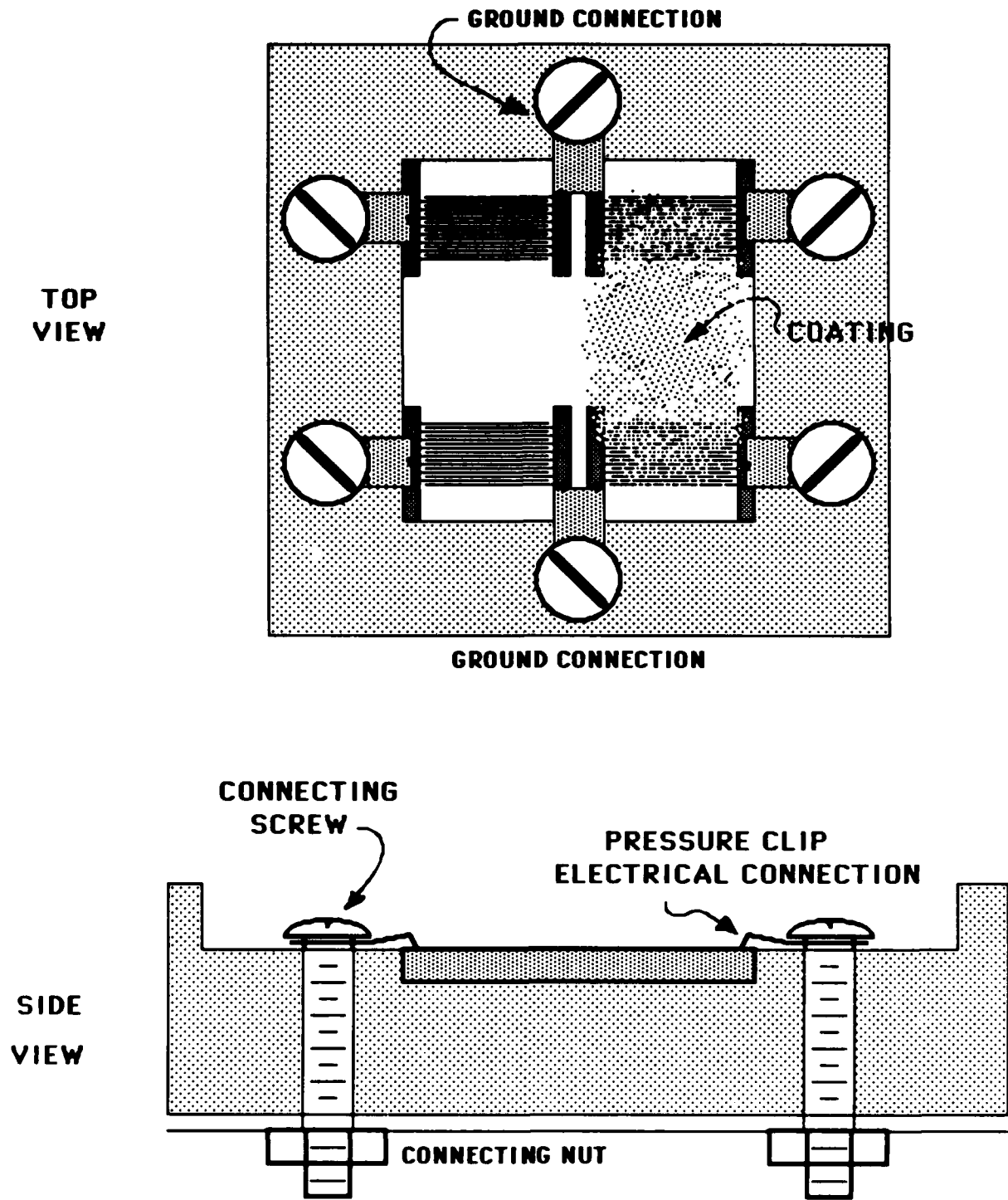


Figure 2. Schematic diagram of a coated 112 MHz dual SAW delay line contained in a plastic box with electrical connections made by screws and pressure clips.

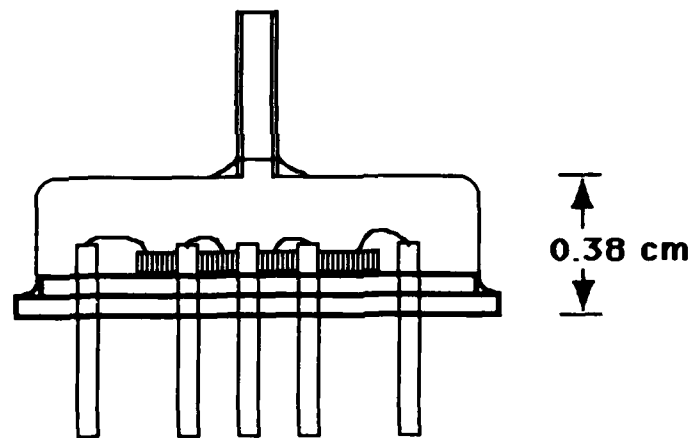
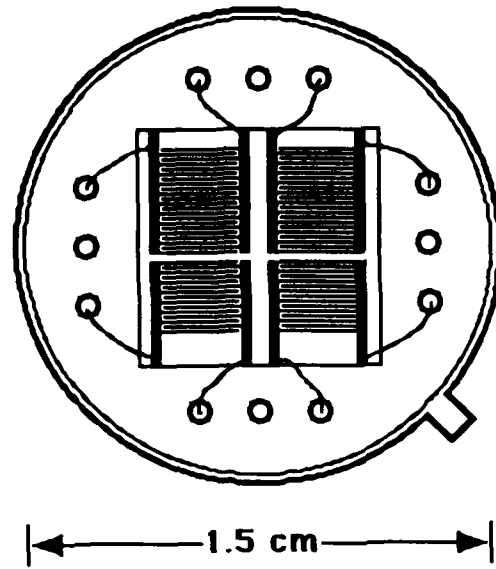


Figure 3. Schematic diagram of a 158 MHz dual SAW delay line mounted on a TO-8 style package with wire-bonded electrical connections.

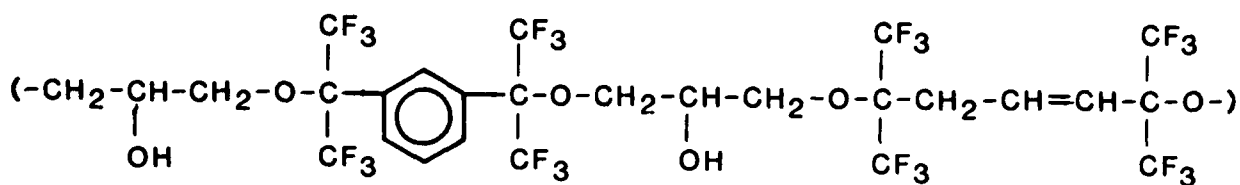


Figure 4. The structure of fluoropolyol.

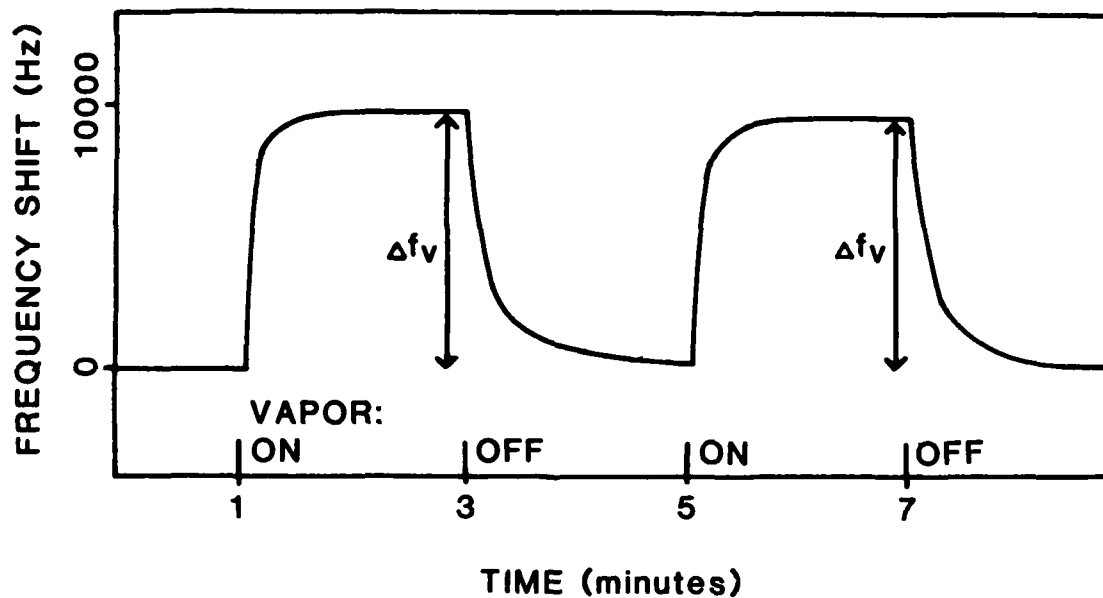


Figure 5. Response curve from two successive exposures of the 158 MHz SAW sensor to N,N-dimethylacetamide at $.000057 \text{ g L}^{-1}$ gas phase concentration.

vapors such as dimethyl methylphosphonate (DMMP) frequency shifts as high as five to ten thousand Hz were observed. Similarly, shifts for 2-butanone, whose vapor phase concentration was very high, ranged up to ten thousand Hz. Vapor induced frequency shifts on the order of a few thousand Hz or less are much smaller than the one hundred thousand Hz of fluoropolyol coating on the 112 MHz devices. This demonstrates that the mass loading of the coating by vapor is small, and validates the use of the density term in equation (10).

The two 112 MHz sensors prepared for this study were coated with 106 and 104 KHz of fluoropolyol, and tested against vapor simultaneously by connecting them to the vapor stream in series. Testing began one day after coating the devices, and was repeated two months later to see if aging influenced sensor responses. These two devices differed slightly in their handling between coating and vapor testing. The device with 106 KHz of fluoropolyol was simply stored under ambient air at room temperature. The film on the second device, however, was annealed at 110°C for one hour, and then stored under ambient conditions. For the two months in between vapor testing, these devices were both stored under ambient conditions.

The 158 MHz device was coated with 207 KHz of film and tested a week later. In between coating and testing the device was stored under ambient conditions. The frequency shifts observed for the 158 MHz sensor were typically twice those observed for the corresponding vapor exposures on the 112 MHz sensors. This is due to the presence of twice the amount (in

KHz) of fluoropolyol on this sensor compared to the 112 MHz sensors. These results are in accordance with the linear dependence of Δf_v on Δf_s as expressed in equation (10).

For each vapor exposure, a partition coefficient was calculated from the observed frequency shift using equation (10). These values will be referred to as SAW partition coefficients and denoted K_{SAW} . The logarithms of the K_{SAW} values for a given vapor were then averaged. Average $\log K_{SAW}$ values are reported in Tables I through V for fluoropolyol on a 112 MHz device one day after coating, annealed fluoropolyol on a 112 MHz device one day after coating, fluoropolyol on a 112 MHz device two months after coating, annealed fluoropolyol on a 112 MHz device two months after coating, and fluoropolyol on a 150 MHz device one week after coating. Also reported with each $\log K_{SAW}$ value are the standard deviation (S), the number of vapor exposures used to determine K_{SAW} values (N), the number of different concentrations for each vapor (#), and the vapor concentration range. These tables represent nearly 900 measurements of SAW frequency shifts.

For the vapors and concentrations examined in this study, the frequency shifts observed increased linearly with vapor concentration, and K_{SAW} values were independent of vapor concentration. This is in accordance with the relationships expressed in equation (10). Graphically this corresponds to a linear calibration curve of SAW response vs. concentration whose slope is dependent on a constant partition coefficient.

Table I. Average Log KSAW Values for 106 KHz of Fluoropolyol
on a 112 MHz SAW Device One Day After Coating Application

VAPOR	Log KSAW	Sa	Nb	#C	Concentration Range, g/l
DMMP	(6.56) ^d	.15	38	7	3.59E-6 2.63E-5
N,N-Dimethylacetamide	(6.30)	.05	40	7	7.47E-6 5.47E-5
1,2-Dichloroethane	2.52	.06	16	4	.0182 .124
Toluene	2.74	.06	16	4	.00625 .0434
Isooctane	2.11	.06	8	2	.0454 .0914
Diethyl sulfide	2.82	.05	16	4	.00797 .0552
2-Butanone	3.12	.02	16	4	.0145 .0986
Water	3.04	.04	8	2	.00271 .00550
1-Butanol	3.20	.03	12	3	.00205 .00815

a S = standard deviation

b N = number of measurements

c # = number of different concentrations

d values in parantheses are less certain. See experimental section.

Table II. Average Log KSAW Values for 104 KHZ of Annealed Fluoropolyol on a 112 MHz SAW Device One Day After Coating Application

VAPOR	Log KSAW	Sa	Nb	#C	Concentration Range, g/l
DMMP	(6.36) ^d	.07	40	7	3.59E-6 2.63E-5
N,N-Dimethylacetamide	(6.10)	.08	40	7	7.47E-6 5.47E-5
1,2-Dichloroethane	2.30	.06	16	4	.0182 .124
Toluene	2.62	.05	16	4	.00625 .0434
Isooctane	2.00	.04	8	2	.0454 .0914
Diethyl sulfide	2.65	.10	16	4	.00797 .0552
2-Butanone	2.98	.02	16	4	.0145 .0986
Water	2.49	.11	8	2	.00271 .00550
1-Butanol	3.16	.02	12	3	.00205 .00815

aS = standard deviation

bN = number of measurements

c# = number of different concentrations

d values in parentheses are less certain. See experimental section.

Table III. Average Log KSAW Values for 106 KHz of Fluoropolyol
 on a 112 MHz SAW Device Two Months After Device Coating

VAPOR	Log KSAW	s _a	n _b	#c	Concentration Range, g/l
DMMP	5.69	.05	36	6	6.83E-5 1.59E-4
N,N-Dimethylacetamide	5.50	.06	44	7	1.38E-5 1.01E-4
1,2-Dichloroethane	2.33	.08	16	4	.0182 .151
Toluene	2.65	.09	16	4	.00731 .0652
Isooctane	1.88	.05	12	3	.0454 .137
Diethyl sulfide	2.72	.06	16	4	.00933 .0820
2-Butanone	3.12	.09	16	4	.0169 .146
Water	2.91	.05	12	3	.00271 .00827
1-Butanol	3.25	.02	16	4	.00136 .0123

s_a = standard deviation

n_b = number of measurements

#c = number of different concentrations

Table IV. Average Log KSAW Values for 104 KHZ of Annealed Fluoropolyol on a 112 MHZ SAW Device Two Months After Coating Application

VAPOR	Log KSAW	s _a	N _b	#C	Concentration Range, g/l
DMMP	5.60	.04	36	6	5.15E-5 1.59E-4
N,N-Dimethylacetamide	5.39	.04	40	7	1.30E-5 1.01E-4
1,2-Dichloroethane	2.20	.06	16	4	.0182 .151
Toluene	2.50	.08	16	4	.00731 .0652
Isooctane	1.70	.03	12	3	.0454 .137
Diethyl sulfide	2.62	.08	16	4	.00933 .0828
2-Butanone	3.00	.06	16	4	.0169 .146
Water	2.04	.07	12	3	.00271 .00827
1-Butanol	3.10	.01	12	3	.00401 .0123

s_a = standard deviation

N_b = number of measurements

#C = number of different concentrations

Table V. Average Log KSAW Values for 207 KHz of Fluoropolyol
on a 158 MHz SAW Device One Week After Coating Application

VAPOR	Log KSAW	sa	Nb	#c	Concentration Range, g/l
DMMPd	6.02	.15	54	7	4.86E-5 3.56E-4
N,N-Dimethylacetamide	6.05	.07	47	7	1.26E-5 1.10E-4
1,2-Dichloroethane	2.59	.09	16	4	.0182 .124
Toluene	2.93	.06	15	4	.00625 .0434
Isooctane	2.16	.09	16	4	.0132 .0914
Diethyl sulfide	3.10	.05	16	4	.00797 .0552
2-Butanone	3.52	.06	16	4	.0145 .0986
Water	3.11	.06	15	4	7.88E-4 .00550
1-Butanol	3.68	.05	16	4	.00116 .00815

aS = standard deviation

bN = number of measurements

c# = number of different concentrations

d Log K values for DMMP showed a systematic decrease with increasing vapor concentration i.e. the calibration curve was not linear.

Alternatively stated, the sorption isotherms were linear in the concentration ranges examined. The principle exception to this rule was DMMP on the 150 MHz device. A slight decrease in K_{SAW} with increasing concentration was observed in this data set.

The reproducibility of a given SAW sensor tested one day after coating and again two months after coating was good, and aging appeared to have little effect. Average $\log K_{SAW}$ values had standard deviations up to about 0.1 $\log K$ units, whereas the differences between values from one day to two months were generally 0 to 0.2 $\log K$ units. Variations for water and isooctane were somewhat greater, but these are vapors to which fluoropolyol is not very sensitive at the vapor concentrations generated.

Data from device to device showed some systematic variations. In testing both one day and two months after coating, the 112 MHz SAW device with the annealed film was about 0.1 to 0.2 $\log K$ units less sensitive than the unannealed film on a 112 MHz device. (The data for water were anomalous.) This systematic variation is small, and may or may not be an effect of annealing the film. The $\log K_{SAW}$ values determined from the data collected on the 150 MHz device are systematically higher than those from 112 MHz device data by about 0.4 $\log K$ units. Systematic variations from device to device could be most easily explained by errors in the measurement of the coating material applied, or by differences in the temperatures at which the sensors were operating during testing. Temperature effects will be further discussed below.

K Values Determined by GLC Measurements. Partition coefficients for a wide variety of solute vapors were determined by gas-liquid chromatography using fluoropolyol as the stationary phase. Partition coefficients as defined in equation (3) are actually identical to the Ostwald solubility coefficients usually denoted as L. We will continue to use the symbol K, and refer to GLC partition coefficients as K_{GLC} . The absolute values of K determined for the alcohols used as standard solutes (see Experimental section for details) are presented in Table VI.

In general, the GLC peaks on the fluoropolyol at 298°K were broad and precise retention volumes (and hence K_{GLC}) were difficult to determine at this temperature. Therefore, 26 K_{GLC} values were determined at both 298°K and 333°K and the following correlation was found to hold:

$$\log K_{GLC}(298K) = -0.728 + 1.470 \log K_{GLC}(333K) \quad (14)$$
$$n = 26, sd = 0.156, r = 0.986$$

When retention times were too long to measure at 298°K, equation (14) and the measured value of K_{GLC} at 333°K were used to estimate the value of K_{GLC} at 298°K.

Standard deviations were not obtained for all the solutes examined. However, the results in Table VI indicate that the probable error on the $\log K_{GLC}$ values will usually not be larger than 0.01 log units. For solutes with very large $\log K_{GLC}$ values, the error may be somewhat larger.

Table VI. Absolute Values of K Determined by GLC. a

Solute	298°K		333°K	
	Value	Deviation	Value	Deviation
Methanol	579.6	± 11.7 (7)	170.0	± 1.4 (3)
Ethanol	728.2	± 12.7 (6)	246.4	± 6.0 (3)
1-Propanol	2174.8	± 22.0 (5)	445.9	± 2.6 (3)
1-Butanol	6975.2	± 37.1 (4)	961.2	± 4.5 (5)
1-Pentanol			2035.8	± 34.4 (5)
1-Hexanol			4203.8	± 14.0 (5)

a Standard deviations are given. The values in parenthesis are the number of determinations.

Log K_{GLC} and log K_{SAW} values for nine solute vapors are compared in Table VII with vapors in order of decreasing log K_{SAW} . All of the GLC values refer to 298°K, either by direct measurement, or via equation (14) as described above. In one additional case, diethyl sulfide, the log K_{GLC} value was estimated from various correlations we have constructed using solvatochromic parameters. With the exception of this estimated value, the order of decreasing log K values is identical for the SAW and GLC measurements. Indeed, there is good agreement between all but the highest log K values, such that the SAW sensor frequency shifts could be estimated using K_{GLC} values and equation (10). The general trend of the highest Log K vapors (DMMP and dimethylacetamide) having larger SAW responses than the other vapors could also be predicted from K_{GLC} , but not accurately. In these cases, the error in Log K_{GLC} values will be larger than usual, but certainly not so large to account for the differences in Table VII.

DISCUSSION

The experimental conditions for measuring partition coefficients with a SAW device are somewhat different than those for GLC measurements. SAW measurements, for instance, are carried out at finite vapor concentrations while the GLC measurement usually refers to infinite dilution. In addition, the SAW measurements reported here were conducted at ambient temperatures, while the GLC measurements were rigorously thermostatted. Finally, the calculation of K_{SAW} assumes that

Table VII. Comparison of Log KSAW and Log KGLC Values

VAPORS	Log KSAW	Log KGLC
Dimethyl methylphosphonate	5.77	7.53C
N,N-Dimethylacetamide	5.65	7.29C
1-Butanol	3.24	3.66
2-Butanone	3.15	3.48C
Water	2.88	2.89
Diethyl sulfide	2.78	2.54d
Toluene	2.69	2.64C
1,2-Dichloroethane	2.39	1.94C
Isooctane	1.97	1.22

a These values are averages of those in Table I-V, excluding values which are in parentheses.

b At 298°K.

c Determined from values measured at 333°K and corrected to 298°K with equation (9).

d Estimated value using a correlation equation.

the vapor causes the sensor to respond based on mass effects alone; if mechanical effects become significant for a particular vapor/coating interaction, then the calculated K_{SAW} will be altered proportionately. One or more of the above factors may be responsible for differences in the precise values of $\log K_{SAW}$ and $\log K_{GLC}$ shown in Table VII. In this regard, the standard deviations reported with the $\log K_{SAW}$ values in Tables I-V represent the variation of the measurement about some value which may or may not be the same as the fluoropolyol/gas partition coefficient at infinite dilution.

The influence of temperature on partition coefficients deserves some attention. It is well known from GLC that increasing temperature causes smaller retention volumes and lower partition coefficients. Consequently a SAW sensor will become less sensitive as temperature increases. The extent of this effect for fluoropolyol is now experimentally defined by the results in Table VI and equation (14). Precise thermostating of a SAW device to fractions of a degree is clearly not critical, but changes of five to ten degrees will influence sensor response and reproducibility, especially for strongly sorbed vapors.

In practice, an unthermostatted sensor may change temperature because of changing ambient conditions, or because the electronics package containing the sensor generates heat. In our experience, the system containing the 158 MHz SAW sensors heats up to the 35 to 40° range, while temperatures as high as 55° have been measured in the 112 MHz SAW sensors systems we have

used. The worst case effect of these temperatures can be illustrated for DMMP, with $\log K_{GLC} = 7.5$ at 298°K . From equation (14) it is estimated that $\log K$ at 40°C will be 6.7, and at 55°C only 5.9. These higher temperature estimates are closer to the results observed experimentally for the SAW sensors. The effect is much less severe for vapors with lower K values. Thus, a $\log K$ of 3.0 at 298°C becomes 2.8 at 40°C and 2.6 at 55°C . The influence of temperature on K values and the higher operating temperatures of our sensors may explain the discrepancy observed between $\log K_{GLC}$ and $\log K_{SAW}$ for strongly sorbed vapors (DMMP and dimethylacetamide), while less strongly sorbed vapors are in better agreement. In addition, temperature effects may also contribute to the higher K values observed for the 158 MHz sensor compared to the 112 MHz sensors.

The overall correlation between K_{GLC} and K_{SAW} values clearly shows that partition coefficients are a useful concept for thinking about SAW sensor behavior (see also references 3 and 7). Indeed, the calculation of K_{SAW} values by equation (10) provides a standardized method of normalizing empirical SAW data which also provides information about the magnitude of the vapor/coating interaction. We have previously normalized our data by dividing the sensor response by the ppm of vapor in the gas phase and the KHz of coating.³ Normalization to yield a partition coefficient, K_{SAW} , is very similar, and requires only that the vapor concentration be expressed in g liter^{-1} , and that the density of the stationary phase coating be factored out,

according to equation (10). Expressing vapor concentration in the international convention of mg m^3 instead of g liter^{-1} requires only a simple conversion factor of 10^6 .

The correlation between K_{GLC} and K_{SAW} is important because it demonstrates experimentally that relative retention times for various vapors on a GLC column with a given stationary phase should be a reliable indicator of the relative sensitivity of a similarly coated SAW sensor to these vapors. This requires, of course, that the GLC measurement and SAW device operation be at the same temperature. On a more quantitative level, if absolute K_{GLC} values are determined, then estimates for actual SAW sensor frequency shifts can be made using equation (10). Finally, a clear relationship between SAW sensor responses and K_{GLC} values means that methods developed to predict K_{GLC} values will also be useful in predicting SAW sensor responses.

The correlation between the K_{GLC} and K_{SAW} values also provides important confirmation of the general operating principles of coated SAW chemical sensors. The functioning of the device primarily as a mass sensor is confirmed because mass sensitivity was a fundamental assumption of the equation used to calculate the K_{SAW} values. In addition, the concept of reversible partitioning of the vapor between the gas phase and the stationary phase is clearly demonstrated. Since partitioning represents the dissolution of a solute vapor into a solvent stationary phase, the solubility model for SAW coating/vapor

interactions is confirmed, and solubility interactions are indicated as important factors in determining sensor responses.³

A simple examination of the order of the partition coefficients determined in this study further illustrates the importance of solubility properties (Table VII). The lowest K values are those of isooctane, a solute which is not dipolar or polarizable, and which cannot accept or donate hydrogen bonds. Solutes which are more polarizable, such as dichloroethane, toluene, and diethyl sulfide have greater K values than isooctane. However, these solutes are still incapable of hydrogen bonding. The top of the list contains exclusively those solutes which can accept and/or donate hydrogen bonds.

A further influence on the order of vapor sorption is the saturation vapor pressure of the solute, P_v^0 . Values of K_{GLC} are proportional to solute adjusted retention times. All other things being equal, solutes of low P_v^0 values will be eluted after more volatile solutes, and hence in general will have larger K_{GLC} values and will give rise to larger Δf_v values in equation (10). Experimentally, this result is seen in the high frequency shifts and K values seen for DMMP. This solute has a vapor pressure of less than 1 Torr at room temperature.

Solubility interactions can be placed on a more quantitative scale by the use of solvatochromic parameters, which describe the dipolar and hydrogen bonding properties of the solute vapors.^{14,15} Such parameters are available for a wide range of vapors, but similar parameters are not yet available

for very many coating materials. The challenges, therefore, are to characterize the solubility properties of polymeric stationary phases, and ultimately to be able to predict partition coefficients for any vapor with any characterized phase. Methodologies to accomplish this are being developed using equations of the general form shown in equation (15).¹⁶

$$\log K = \text{constant} + S\pi^* + a\alpha + b\beta + l \log L^{16} \quad (15)$$

In this equation, the parameters π^* , α , β , and $\log L^{16}$ characterize the solute vapor. The first three measure the dipolarity, hydrogen bond donor acidity, and hydrogen bond acceptor basicity, respectively. L^{16} is the Ostwald solubility coefficient (partition coefficient) of the solute vapor on hexadecane at 25°C. The coefficients s , a , b , and l are determined by multiple regression analysis and characterize the stationary phase. For example, b , as the coefficient for solute hydrogen bond acceptor basicity, provides a measure of the stationary phase hydrogen bond donor acidity. For any particular stationary phase/vapor interaction, evaluation of the individual terms (such as $b\beta$) and comparison of their magnitudes allows the relative strengths of various solubility interactions to be sorted out and examined.

The complex structure of fluoropolyol provides an interesting test case for these methods. This polymer contains a variety of functionalities which provide polarizability, dipolarity, hydrogen bond acceptor sites, and hydrogen bond

donor sites. But the structure alone does not allow precise predictions of which interactions will be most important in determining the sorption of a particular vapor. Full characterization of fluoropolyol by GLC measurements and equations of the form in (15) is in progress, and we hope to report on this work soon. In addition, various other polymeric stationary phases which have been useful as SAW sensor coatings are being examined. Once the coefficients for a given phase have been determined, then it will be possible to evaluate solubility interactions and to predict K values for all vapors for which the relevant solute parameters are known. Then, via equation (10), it will be possible to predict the responses of a SAW vapor sensor to the same set of vapors.

Finally, it is anticipated that specific vapor/coating interactions may be encountered where mass effects alone do not adequately account for SAW sensor response. In such cases, mechanical effects (e.g. stiffening or softening of the surface coating by penetrant vapor) will be implicated, and the relationship between the actual coating/gas partition coefficient and SAW frequency shift will not be so simple as that expressed in equation (10). However, equation (10) will allow the frequency shift due to mass effects alone to be estimated if the partition coefficient has been measured by GLC or if it can be predicted from solubility parameters. It will then be possible to estimate the mechanical effect from the difference between the observed frequency shift and the frequency shift due to mass effects calculated from equation (10). Therefore, equation (10)

will be useful for predicting SAW sensor responses when mass effects predominate, and in sorting out mass and mechanical effects when mass changes alone do not account for observed behavior.

CONCLUSIONS

An equation has been derived which relates SAW vapor sensor frequency shifts directly to partition coefficients. This equation has been validated by a comparison and correlation of partition coefficients determined independently by SAW vapor sensor responses and GLC measurements. This correlation also confirms mass sensitivity as the principle mechanism of vapor sensitivity for fluoropolyol-coated vapor sensors, and reversible sorption as the mechanism of vapor/coating interaction. Solubility properties such as dipolarity and hydrogen bonding are indicated as important factors in determining the extent of vapor sorption. The saturation vapor pressure of the solute vapor also influences sorption. The direct relationship between SAW sensor response and partition coefficients provides an avenue for predicting SAW sensor response from measured GLC partition coefficients. Partition coefficients predicted from solute vapor solvatochromic parameters and correlation equations characterizing the solvent stationary phase are also expected to be useful for predicting SAW sensor responses.

ACKNOWLEDGEMENTS

The authors acknowledge M.J. Kamlet for many useful discussions on solubility interactions.

This work was supported by the U.S. Army, CRDEC, Aberdeen Proving Ground, MD, and the U.S. Navy, Naval Surface Weapons Center, Dahlgren, VA and the Office of Naval Technology.

REFERENCES

1. Wohltjen, H.; Dessy, R.E., Anal. Chem., 1979, 51, 1458-1475.
2. Wohltjen, H.; Snow, A.W.; Barqer, W.R.; Ballantine, D.S., IEEE Trans. Ultrason., Ferroelectrics, Freq. Contr., in press.
3. Ballantine, D.S.; Rose, S.L.; Grate, J.W.; Wohltjen, H., Anal. Chem., 1986, 58, 3058-3066.
4. Wohltjen, H.; Snow, A.; Ballantine, D., Proc. of the Int. Conf. on Solid State Sensors and Actuators - Transducers '85, Philadelphia, PA, June 11-14, 1985, IEEE Cat. No. CH2127-9/85/0000-0066, pp 66-70.
5. Venema, A.; Nieuwkoop, E.; Vellekoop, M.J.; Nieuwenhuizen, M.S.; Barendsz, A.W., Sens. Actuators, 1986, 10, 47-64
6. Wohltjen, H. Sens. Actuators, 1984, 5, 307.
7. Snow, A.; Wohltjen, H. Anal. Chem., 1984, 56, 1411.
8. Bryant, A.; Poirier, M.; Riley, G; Lee, D.L.; Vetelino, J.F., Sens. Actuators, 1983, 4, 105.

9. D'Amico, A.; Palma, A.; Verona, E., Sens. Actuators, 1982/1983, 3, 31.
10. Chuanq, C.T.; White, R.M.; Bernstein, J.J., IEEE Electron, Device Lett., 1982, 3(6), 145.
11. O'Rear, J.G.; Griffith, J.R.; Reines, S.A., J. Paint. Technol., 1971, 43(552), 113.
12. Grate, J.W.; Ballantine, D.S., Jr.; Wohltjen, H., Sens. Actuators, 1987, 11, 173-188.
13. Abraham, M.H.; Grellier, P.L.; McGill, R.A., J. Chem. Soc. Perkin Trans. I, in press.
14. Kamlet, M.J.,; Taft, R.W., Acta Chem. Scand., Ser. B, 1985, B39, 611, and references therein.
15. Kamlet, M.J.; Abboud, J.M.; Abraham, M.H.; Taft, R.W., J. Org. Chem., 1983, 48, 2877.
16. Abraham, M.H.; Grellier, P.L.; McGill, R.A.; Doherty, R.M.; Kamlet, M.J.; Hall, T.M.; Taft, R.W.; Carr, P.W.; Koros, W.J., Polymer, in press.

APPENDIX

Relationships to Henry's Law Constants and Activity Coefficients

The Henry's Law constant, K^H , is defined as the ratio of the partial pressure of the solute vapor in the gas phase, P_V , to the mole fraction of the solute vapor in the liquid phase (equation 16).

$$K^H = \frac{P_V}{x_S} \quad (16)$$

This law applies to the limiting case of dilute solutions, where x_S approaches zero. Activity coefficients, γ , are defined according to equation (17), and K^H and γ are related by equation (18).

$$P_V = \gamma x_S P_V^\circ \quad (17)$$

$$K^H = \gamma P_V^\circ \quad (18)$$

P_V° is the saturation vapor pressure of the vapor at the experimental temperature.

Both K^H and γ can be related to the partition coefficient, K , if additional assumptions are made. SAW frequency shifts can then be calculated as well. If the vapor is assumed to behave ideally in the gas phase, then P_V (in atm.) is simply related to C_V (in g liter⁻¹) by equation (19).

$$P_V = \frac{C_V RT}{M_V} \quad (19)$$

M_v is the molecular weight of vapor. The ratio of the moles of solute vapor in the stationary phase to the moles of solvent molecules in the stationary phase can be determined from C_s using the density of the stationary phase and its molecular weight, ρ and M_s , respectively. For the case of very dilute solutions, the mole fraction of the vapor in the stationary phase, x_s , will be nearly equivalent to their mole ratio, i.e. the moles of solute vapor is much less than the moles of solvent. The mole fraction can be expressed as in equation (20).

$$x_s \approx \frac{C_s M_s (.001 \text{ kg g}^{-1})}{M_v \rho} \quad (20)$$

Finally, division of equation (19) by equation (20) gives the Henry's law constant as defined in equation (16). Substitution of the definition of K (equation 3) and rearranging then relates K^H to K in equation (21).

$$K = \frac{1}{K^H} \frac{R T \rho}{M_s (.001 \text{ kg/g})} \quad (21)$$

Similarly, K and γ are related by equation (22)

$$K = \frac{1}{\gamma} \frac{R T \rho}{P_v^0 M_s (.001 \text{ kg/g})} \quad (22)$$

Equations (21) and (22) can easily be substituted into equation (9) so that SAW sensor frequency shifts can be calculated if K^H or γ is known for the interaction between the

vapor and the stationary phase coating at a relevant temperature and vapor concentration. By using equation (19) as well as equations (9) and (22), Δf_v is related to γ by equation (23).

$$\Delta f_v = \Delta f_s \frac{P_v}{P_v^0} \frac{M_v}{M_s} \frac{1}{\gamma} \quad (23)$$

Equation (23) differs from equation (10) in several ways. The density term and the assumptions associated with it in equation (10) have been cancelled out of equation (23). The most convenient units for Δf_s in equation (23) are Hz and the equation is expressed in this form. The vapor concentration in the vapor phase is expressed in partial pressure. However, equation (23) is rigorously correct only for liquid stationary phases whose molecular weight is known. It is awkward for polymeric stationary phases. Moreover, activity coefficients refer primarily to the interaction between the liquid vapor and the liquid stationary phase, while we are more interested in the equilibrium between the gaseous vapor and the liquid stationary phase.

The terms in equation (23) show that SAW frequency shifts (Δf_v) will increase with decreasing saturation vapor pressure (P_v^0) of the solute vapor. This result is consistent with the known increases in GLC retention times and partition coefficients with P_v^0 . Equation (23) also suggests that the molecular weight of the stationary phase (M_s) will influence Δf_v . However, changes in M_s are cancelled out by corresponding

changes in γ because γ depends on molar volume. Thus, GLC experiments have demonstrated that retention volumes (and therefore partition coefficients) show little change with variations in stationary phase molecular weight.

END

9-87

DTIC